

**UCRL-JC-152221**

**Title:** Gene expression changes in mouse brain after exposure to low-dose ionizing radiation.

Eric Yin<sup>1</sup>, David O. Nelson<sup>1</sup>, Matthew A. Coleman<sup>1</sup>, Leif E. Peterson<sup>2</sup>, Andrew J. Wyrobek<sup>1\*</sup>

<sup>1</sup>Biology and Biotechnology Research Program, Lawrence Livermore National Laboratory, Livermore, CA 94550

<sup>2</sup>Department of Medicine, Baylor College of Medicine, Houston, TX 77030

\*Corresponding author:

Andrew J. Wyrobek, Ph.D.

Biology and Biotechnology Research Program

Lawrence Livermore National Laboratory

P.O. Box 808 L-448

Livermore, CA 94550

Telephone: (925) 422-6296

Fax: (925) 424-3130

E-mail: wyrobek1@llnl.gov

**Keywords:** ionizing radiation, low-dose, gene expression, oligonucleotide microarray

## **Abstract.**

*Purpose:* Characterize the cellular functions associated with the altered transcript profiles of mouse brain exposed to low-dose in vivo gamma irradiation . *Materials and methods:* Cerebral RNA was isolated at 30 minutes and 4 hours after whole-body irradiation at 0.1 Gy or 2 Gy, hybridized to random oligonucleotide arrays, and evaluated for time and dose response patterns by multifactorial analyses. *Results:* Brain irradiation modulated the expression patterns of 1574 genes, of which 855 showed more than 1.5 fold variation. ~30% of genes showed dose-dependent variations, including genes exclusively affected by 0.1 Gy. ~60% of genes showed time-dependent variation with more genes affected at 30 minutes than 4 hours. Early changes involved signal transduction, ion regulation and synaptic signaling. Later changes involved metabolic functions including myelin and protein synthesis. Low-dose radiation also modulated the expression of genes involved in stress response, cell-cycle control, and DNA synthesis/repair. *Conclusions:* Doses of 0.1 Gy induced changes in gene expression that were qualitatively different from those at 2 Gy. Our findings suggest that low-dose irradiation of the brain induces the expression of genes involved in protective and reparative functions while down-modulating genes involved in neural signaling activity.

## Introduction

Exposure of cells to ionizing radiation (IR) results in damage to cellular organelles, membranes, and biomolecules through direct energy deposition and generation of toxic radicals (Somaso 2000, Tofilon and Fike 2000), resulting in diverse cellular outcomes across tissues and cell types. The adult brain has been considered insensitive to IR, due to the relatively radioresistant nature of neurons (Belka et al. 2001), which in some model systems show no signs of injury after exposures of up to 15 Gy (Tofilon and Fike 2000). At high doses, IR can induce acute effects such as edema and inflammation from vascular damage (Hopewell and Wright 1970), with concomitant clinical symptoms of nausea, emesis and fatigue (Anno et al. 1989). High dose IR can also induce demyelination and neuronal loss (van der Kogel 1983), with associated neural and cognitive deficiencies (Abayomi 2002). However, the molecular mechanisms underlying the cellular changes in the irradiated brain have not been well characterized.

Gene expression changes have been reported after IR exposure of the brain, but generally only at relatively high doses ( $\geq 7$  Gy), and utilizing single-gene analysis methods. Such high-dose exposures induced genes involved in early signal transduction events (Ogawa et al. 1996, Usenius et al. 1996, Hong et al. 1997), inflammation (Hong et al. 1995, Chiang et al. 1997, Raju et al. 1999, Kim et al. 2002,), and apoptosis (Ferrer et al. 1995). However, little information exists on the *in vivo* effects of low-dose irradiation ( $\leq 0.1$  Gy) of the brain. Evidence from studies of myeloid lymphoblastoid cell lines suggest that the transcriptional response at lower doses may differ qualitatively as well as

quantitatively from that of higher doses (Amundson et al. 2001). In addition, recent studies of mice receiving IR doses as low as 0.01 Gy noted that both radiosensitive and radioresistant tissues exhibited changes in the expression of Trp53, which plays a central role in both DNA damage and stress response by selecting downstream effectors for proliferation or apoptosis. There was no apparent lower threshold of induction (MacCallum et al. 2001) raising the possibility that IR effects could also occur in the brain at low doses.

DNA microarray technology provides a means of evaluating the relative expression of thousands of genes in parallel, and has been used to characterize transcript profiles for various regions of the adult brain (Serafini 1999, Cao and Dulac 2001). In our study, we employed large-scale random oligonucleotide microarrays to characterize transcript profiles of the brain tissue of adult male mice at 30 minutes and 4 hours after exposure to 0.1 Gy or 2 Gy of IR. The 2 Gy dose is at the lower end of the range for doses used in prior studies with adult mice and is within the range of daily doses used in brain radiotherapy, while the 0.1 Gy dose is substantially lower. Our research addresses the following questions: i) does 0.1 Gy IR elicit genome scale gene expression changes in the adult mouse brain? ii) how do low-dose effects differ from those of a higher dose? iii) how do the time-response patterns vary up to 4 hours after irradiation? and iv) what are the possible cellular functions associated with IR-modulated genes? Our approach provides an unbiased description of the molecular and cellular mechanisms employed by the brain after low-dose IR exposure, and provides new insight into understanding the potential health consequences of low-dose exposure.

## **Materials and Methods**

### **Mice**

Eight to ten-week old male B6C3F1/HSD mice were exposed to whole-body irradiation of either 0.1 Gy (n = 4) or 2 Gy (n = 4) of gamma-radiation using a  $^{137}\text{Cs}$  source with 5x attenuation at a dose rate of 0.64 Gy/minute. Two groups of six mice were sham irradiated for use as control reference groups, to improve the representation of the average value for this hybrid line. Two animals from each radiation exposure group were euthanized with  $\text{CO}_2$  at 30 minutes post-irradiation. The remaining animals, including controls were euthanized at 4 hours. Brains were surgically removed and frozen on dry ice. Based on brain morphology, a coronal section of the cerebrum from the anterior of the septo-diencephalon to the posterior of the diencephalon was isolated for analysis using a surgical scalpel. This section included the motor cortex, portions of the frontal and parietal lobes, hippocampus, and diencephalon. Coordinates for the section corresponded to regions 205-305 from the High Resolution Mouse Brain Atlas (<http://www.hms.harvard.edu/research/brain/atlas.html>). RNA was prepared from the sections, which varied from 100-150 mg, using Trizol (Life Technologies, Rockville, MD), followed by DNase treatment and RNeasy (Qiagen, Valencia, CA) column purification. Procedures for handling mice conformed to IACUC guidelines at Lawrence Livermore National Laboratory.

### **Oligonucleotide Microarrays**

Brain RNA from individual irradiated animals was evaluated for changes in expression against pooled brain RNA from control animals. Probe preparation, hybridization, and image capture was performed using the Affymetrix system, as described in the Expression Analysis Technical Manual (Affymetrix, Santa Clara, CA). Briefly, RNA probes were generated starting with 5 ug of total RNA from irradiated and pooled control animals. RNA was reverse transcribed using Superscript II reverse transcriptase (Life Technologies, Rockville, MD) and an oligo-dT primer encoding a T7 polymerase binding site 5'-GGCCAGTGAATTGTAATACGACTCACTATAGGGAGGCGG(T)-24-3'). After second strand synthesis, the cDNA was used as template for *in vitro* transcription with the Enzo BioArray HighYield Transcript Kit (Enzo Biochem, New York, NY). A total of 15 ug of the resultant complementary RNA was hybridized to Affymetrix U74A GeneChips®. Samples were incubated at 42 °C for 16 hrs rotating at 60 rpm. After hybridization, chips were washed and developed for detection with the Affymetrix Fluidics Workstation. Signals were detected through the use of an argon-ion laser scanner (Agilent, Palo Alto, CA), and output for pixel intensities and confidence calls for each of the genes detected on the array were generated with Affymetrix Microarray Suite 5 (MAS-5).

### **Statistical Analysis**

Affymetrix oligonucleotide arrays represent genes with 16-20 pairs of 25-mers referred to as a probe set. Each pair consists of a perfect match probe and a mismatch probe used to correct for non-specific binding. Affymetrix MAS-5 analysis software uses scanned intensity values for the probe pairs for a gene to calculate a signal and a p-value

for each gene. The signal is a background-subtracted estimate of signal intensity, while the p-value provides evidence that some specific binding was detected.

The log-transformed signal (base 2) and a p-value fields were used as the source of all raw data for subsequent statistical analyses, which were performed in the statistical computing environment R (Ihaka and Gentleman 1996). All p-values were calculated using the null-hypothesis permutation distribution of the test statistic under consideration (Good 2000). The p-values were transformed to compensate for multiple comparisons using the Benjamini-Hochberg False Discovery Rate (FDR) adjustment procedure described by Dudoit et al. (2002). This adjustment procedure proceeds in three steps. First, the p-values for the  $n$  genes being examined are sorted from smallest to largest, producing sorted p-values  $p_1, p_2, \dots, p_n$ . Second, each sorted p-value is multiplied by an adjustment factor: the smallest p-value  $p_1$  is multiplied by  $n$ , the second smallest by  $n/2$ , the third smallest by  $n/3$ , and so on. Finally, starting with  $p_{n-1}$  and working backwards to  $p_1$ ,  $p_i$  is replaced by the smaller of itself and  $p_{i+1}$ . This p-value adjustment allows us to estimate the average percentage of false positives among genes meeting our criteria for being IR-modulated, since selecting genes based on a threshold for raw p-values can produce gene lists with arbitrarily high or low percentages of false positives.

The log-transformed signals from each hybridization were normalized in three steps. In the first step, genes were selected for normalization if their adjusted Affymetrix p-value was less than 0.01 in at least one hybridization. The p-values for each hybridization were adjusted to ensure a per-hybridization false discovery rate of 1%. The second step of the normalization consisted of normalizing the two replications in each experimental group using Astrand's quantile normalization (Bolstad et al. 2002). In the third step of

normalization, the quantile-normalized, log-transformed signal values from each hybridization were adjusted so that the median signal intensity was the same across all hybridizations.

Genes were evaluated for differential regulation among the five experimental groups using a small modification of the standard F-ratio for testing for differences in a one-way analysis of variance. The modification consisted of replacing the calculated denominator in an F-ratio by the maximum of the denominator for that F-ratio and the median denominator across the F-ratios of all genes evaluated, thus avoiding the selection of genes with artificially low denominators (average within group variance).

Genes with differential group effects detected by F-ratio analysis were then classified into two groups using a saturated linear model for each gene (mean plus dose effect plus time effect plus interaction). Those genes with a significant interaction term, as tested by a permutation test, were not further classified. Each gene with a non-significant interaction term was then evaluated using an additive linear model (mean plus dose effect plus time effect) and classified into one of four groups: i) dose- and time-independent effect, ii) time-dependent effect, iii) dose-dependent effect, and iv) both dose- and time-dependent effects, according to whether or not their dose and/or time terms were significant. These groups consisted of four data points (two representing time, and two representing dose) are referred to as either "response patterns" or "patterns."

The dose effect was calculated by comparing the average of the high-dose effect across the two time points to the average of the low-dose effect across the two time points. The time effect was calculated by comparing the average of the 30 minute effect across the two doses to the average of the 4 hour effect across the two doses. Genes with



significant dose and time terms were combined with the genes with significant interaction terms to obtain a set of complex genes. This complex set was combined with the first three categories of genes with non-significant interaction terms for subsequent analysis (figure 1).

[Insert figure 1 about here]

### **Cluster Analysis**

The set of complex genes was clustered using the Partitioning Around Medoids (PAM) algorithm (Kaufman and Rousseeuw 1990) with a sequence of cluster numbers ranging from two to ten clusters. The validity of each clustering was then evaluated using Pollard's Mean Split Silhouette (Pollard and van der Laan 2002) to generate three clusters for presentation.

A separate cluster analysis using the CLUSFAVOR program (available at <http://mbcr.bcm.tmc.edu/genepi>) was performed to identify natural grouping of genes based on gene expression profiles (Eisen et al. 1998, Sherlock 2000). The underlying metric in this analysis was the concept of geometric distance between pairs of gene expression profiles (Peterson 2002). Clustering was performed on replicate averages of log-transformed (base 2) normalized signal values, selecting parameters for UPGMA (centroid) clustering on objects with 1-correlation as the distance function.

### **Semi-Quantitative PCR**

RT-PCR was performed to validate the microarray results for four IR-modulated genes. Individual reactions were performed using 1 ug of RNA from each sample used for microarray analyses. The RNA was reverse transcribed using Superscript II reverse transcriptase (Life Technologies, Rockville, MD) and an oligo-dT primer. PCR was

performed in 100 ul reactions, using 5 units of HotStar Taq DNA polymerase (Qiagen, Valencia, CA). The *Gapdh* gene, which did not show a change in expression (data not shown), was used as an internal control. The primers selected were as follow: *Gapdh* (0.319 kb) Forward-Primer: CATGGTCTACATGTTCCAGT, Reverse-Primer: GCTGACAATCTTGAGTGAGT; *Csnk2a1* (1.279 kb) Forward-Primer: TTGGTCGGGGCAAGTATAGT, Reverse-Primer: TCAGCTAGTCCTTGGGGTTT; *Pcna* (0.925 kb) Forward-Primer: TTCTGCATCGTGAATCGG, Reverse-Primer: GGCATCTCAGGAGCAATCTT; *Psma4* (0.799 kb) Forward-Primer: TCACCGTCTTCCTCTGGAAT, Reverse-Primer: TTCTTTCTTCTCCCGCTCAG. The following PCR conditions were used for all genes except *Psma4*: 30 cycles at 94°C for 1 minute; 52°C for 1 minute; 72°C for 1 minute, followed by 1 cycle at 72°C for 5 minutes. For *Psma4*, an annealing temperature of 53°C was used.

## Results

Transcription profiles were generated from brain RNA isolated from individual male B6C3F1 mice at 30 minutes and 4 hours after whole-body irradiation at doses of 0.1, or 2 Gy and compared to unirradiated controls. A set of 3517 genes and ESTs (hereafter referred to collectively as genes) had detectable levels of transcript signal in at least one hybridized chip (figure 1). Replicate animals of each experimental group showed a median correlation of 0.94 (range: 0.86 to 0.98). There were 1574 genes which showed an IR effect in at least one treatment group (F-ratio  $p < 0.05$ , FDR = 0.2) (figure 1).

[Insert table 1 about here]

The IR-affected genes were first examined using the simple method of separating genes based on fold-change (table 1). About half were modulated by  $\geq 1.5$ -fold (48% at 30 minutes and 45% 4 hours), while fewer were modulated by more than two-fold (17% at 30 minutes and 11% at 4 hours) or three-fold (4% at 30 minutes and 1% at 4 hours). At 30 minutes there were consistently more genes modulated downward by IR exposure than upward, regardless of fold-change (table 1), a trend that was not as evident at 4 hours.

The IR-responsive genes were then manually assigned to three categories of dose response (table 1). The 0.1 Gy and 2 Gy exclusive categories consisted of genes that met the fold-change threshold for magnitude at one dose of IR, but not the other. Genes that met the fold-change threshold at both doses of IR were placed in the third category. This analysis points to the existence of a substantial fraction of genes that were modulated exclusively at the low dose and not the high dose for both time points (figure 2).

Applying this technique to the analysis of time response showed about 40% of IR-responsive genes overlapped between 30 minutes and 4 hours at either dose (data not shown).

[Insert figure 2 about here]

### **Time- and dose-dependent patterns of expression**

Multifactorial statistical analysis of time- and dose-dependent changes for the 1574 IR responsive genes (see Methods) produced four major expression groups (figure 1), each with multiple patterns (figures 3, 4). Groups 1 and 2 consisted of 1128 genes that showed no statistically significant difference in modulation between the two doses (i.e. they were dose-independent), and represent 70% of all IR-affected genes (figure 1). Group 1 consisted of 225 IR dose-independent genes that also showed no detectable differences in their expression over time. These genes exhibited two types of IR-response patterns (figure 3); increased (figure 3, pattern 1A), and decreased transcript levels (figure 3, pattern 1B) which were sustained over time. Group 2 consisted of 903 dose-independent genes that showed time-dependent changes, that fell into four IR-response patterns (figure 3). Two patterns showed transient changes of expression at 30 minutes that returned toward the baseline by 4 hours (figure 3, patterns 2A, 2B), and two patterns showed IR-modulation at 4 hours but not 30 minutes (figure 3, patterns 2C, 2D).

[Insert figure 3 about here]

Groups 3 and 4 consisted of the remaining 446 genes that showed dose-dependent responses. Group 3 had 77 dose-dependent genes that exhibited no detectable change in expression over time, and fell into four IR-response patterns (figure 3). Two patterns (figure 3, patterns 3A, 3B) included genes for which the effect after 0.1 Gy was greater

than after 2 Gy. Two patterns (figure 3, patterns 3C, 3D) included genes for which modulation after 2 Gy was greater than after 0.1 Gy. Group 4 had 369 genes that showed complex dose and time dependencies that were neither congruent nor parallel. The PAM clustering algorithm was used to group these genes into three patterns of expression (figure 4). Two patterns were time dependent for one dose, but time independent for the other (figure 4, patterns 4A, 4B), and one pattern exhibited inverse time dependency for the two doses (figure 4, pattern 4C). The tables listing the annotated genes in groups 1 to 4 are listed in the supplemental materials (<http://mcg.llnl.gov/external/supplemental/UCRL-JC-152221.htm>).

[Insert figure 4 about here]

### **Functional categories of IR modulated genes**

The set of genes that showed  $\geq 1.5$ -fold changes were selected for assignment to functional categories. Of these 855 genes, only 616 were annotated while 239 were ESTs. We assigned 518 of the annotated genes to specific categories associated with general cell functions (table 2) and neural/glial specific functions (table 3) based on database searches using Unigene, GenBank and other resources at the NCBI website (<http://www.ncbi.nlm.nih.gov>). Genes which exhibited complex patterns of expression were placed into a separate list which combines general and specific functional categories (table 4). With few exceptions, most expression patterns (figure 5) were represented by at least one member from each functional category, suggesting broad involvement of diverse cellular functions in the IR response of the brain.

[Insert figure 5 about here]

[Insert table 2 about here]

[Insert table 3 about here]

[Insert table 4 about here]

In several cases, the majority of genes within a functional category belonged to a single expression pattern, e.g. genes involved in synaptic signaling were primarily modulated downward at 30 minutes (pattern 2B), while protein synthesis and myelin associated genes were primarily increased in expression at 4 hours (pattern 2C). There were also functional categories for which all member genes were consistently modulated in the same direction e.g. decreased expression of motor protein genes at all time points (patterns 2B, 2D, 4A), and decreased expression of neurotrophins (pattern 2B). In general, categories represented at 30 minutes were also represented at 4 hours. However, changes in expression of genes associated with RNA synthesis and modification, DNA repair, cell cycle, heat shock, redox and chromatin structure were primarily seen at 30 minutes after IR exposure (pattern 2A, 2B). Ion regulation, energy metabolism, and signal transduction genes, as well as transcription factors also showed a marked decrease in transcript levels at 30 minutes (pattern 2B).

Four genes were selected for validation by RT-PCR as representatives of separate time- and dose-dependent expression patterns. *Sod1* (data not shown), and *Pcna* (figure 6) were selected as examples of time-dependent genes. RT-PCR confirmed microarray results that both genes showed elevated expression at 30 minutes but not 4 hours. Two dose-dependent genes were also examined. *Csnk2a1* was shown by microarray to be elevated after 2 Gy but not after 0.1 Gy, was confirmed by RT-PCR (figure 6). *Psma4* was shown by microarray to be elevated after 0.1 Gy but not 2 Gy. RT-PCR confirmed

the elevated expression of *Pσμα4* at 4 hours, but the response at 30 minutes remains uncertain (figure 6).

[Insert figure 6 about here]

Cluster analysis was applied to each of the four major groups of genes to identify novel associations between genes in and among functional categories. Clustering showed numerous examples of co-expression among genes that belonged to the same functional category, e.g. redox genes (*Gpx*, *Ggh*),  $\text{Ca}^{2+}$  regulatory genes (*S100a1*, *S100a13*), and synaptic signaling genes (*Syt5*, *Grik5*, *Cck*). Clustering also revealed that genes from different functional categories clustered together e.g. synaptic signaling and signal transduction genes, cell-cycle control and signal transduction genes etc. For example, we found in group 1, the synaptic signaling gene *Grin1* clustered with the signal transduction genes *Prkcc* and *Ptprn*. In group 2, the synaptic signaling genes *Gria3* and *Syt11* clustered with the signal transduction genes *Prkar1b* and *Clk2*. The full cluster analysis images for the four groups are available at the URL:

<http://mcg.llnl.gov/external/supplemental/UCRL-JC-152221.htm>.

## Discussion

We identified 1574 genes in the adult mouse brain that showed statistically significant changes in transcript level after whole-body irradiation at the relatively low doses of 0.1 and 2 Gy of gamma radiation. The magnitudes of transcript changes were correspondingly small (median fold-change  $\sim 1.8$ ), with fewer than 70 genes showing transcript level changes of  $\geq 3$ -fold. By assigning the  $\sim 500$  most highly modulated genes to biochemical pathways and cellular functions, a complex picture emerges of the molecular defense mechanisms employed by brain in response to low-dose irradiation.

IR-exposure induced both quantitative and qualitative responses in the brain. Approximately 70% of modulated genes showed no significant dose response, and of these, over 80% showed time-dependence (figure 3). The existence of so many dose-independent genes suggests that many cellular responses are induced at threshold doses at or below 0.1 Gy, with no further detectable increase with dose. Surprisingly, both the magnitude of change and number of IR-affected genes was generally greater at 0.1 Gy than at 2 Gy. This is particularly evident at the 30 minute time point (table 1, figure 2), and among the time-independent patterns (figure 3, group 3). The 0.1 Gy exclusive genes appear to be involved in a broad variety of cellular functions including catabolism, chromatin structure, signal transduction, vesicle trafficking and synaptic signaling.

Although this is the first genome-scale analyses of the effects of low-dose ionizing radiation on the mammalian brain, there have been prior low-dose reports using single-gene analysis methods. Altered expression of *c-Fos* and *Pomc* was reported after



irradiation of mouse neurons at 0.075 Gy (Wan et al. 2001), but these genes that were not represented on the U74A GeneChips® used in our study. The existence of the 0.1 Gy exclusive genes also suggests that the cellular response mechanisms are qualitatively different at the very low dose, a phenomenon which has been suggested by radiation studies in other systems (Joiner et al. 2001) and raises the questions about how to model risk for adverse health effects for low dose exposure.

We found that low-dose IR exposures modulated genes involved in stress response, synaptic signaling, cell-cycle control and DNA synthesis/repair, suggesting that low-dose IR may activate protective and reparative mechanisms as well as depressing signaling activity. Radiation induced increases in the transcripts of redox genes involved in oxidative stress response e.g. superoxide dismutase and thioredoxin, as well as glutathione pathway genes like glutathione peroxidase, glutathione-S-transferase and glutathione synthetase (table 2, 4). Such genes are believed to be induced as protective measures against reactive oxygen species generated by low-dose IR exposure (Feinendegen 2002), and some have been observed by others at doses in the 0.25 Gy to 0.5 Gy range (Kawakita et al. 2003). Redox genes that were down modulated were part of the mitochondrial cytochrome-c oxidase pathway (e.g. *Cox7a21*, *Cox7c*, *Cyc1*), and may be related to the downward modulation observed for many genes involved in energy metabolism (table 2). The upward modulation of genes for small heat-shock proteins and mitochondrial translocases (table 2) is also consistent with the activation of protective mechanism. Increases in levels of small heat shock proteins (*Dnajc8*, *Dnajb9*) may be related to formation of heat shock granules (HSG) and modulation of chaperone activity (Smykal et al. 2000). Other components of HSGs like actin (*Actb*) and tubulin (*Tuba1*)

also increased in expression (table 2). Large heat shock proteins on the other hand, were down-modulated in our study (table 2). Hsp70 has been demonstrated to increase expression in splenocytes (Kang et al. 2002) and intestinal mucosa (Sonis et al. 2002) of irradiated mice as well as in human tumor cell lines (Stammeler et al. 1996, Ibuki et al. 1998,), but these apparently contradictory results may be related to fundamental differences between in vitro and in vivo exposure biology (Khodarev et al. 2001), or the known differences in the radiosensitivities of the tissues studied. Modulation of mitochondrial translocases like *Tim10* have also been associated with chaperone activity (Vial et al. 2002), and are up modulated in the brain (table 2), consistent with an increase in cellular protective mechanisms. The down-modulation of certain receptor genes involved in synaptic signaling may also be part of a protective mechanism. We observed downward modulation of both AMPA and NMDA receptor transcripts after low-dose irradiation (table 3). Antagonism of AMPA and NMDA receptors have been shown to provide a protective effect in certain neuron populations after ischemia (Pang et al. 2002).

Our findings also suggest that low-dose IR-exposure activated cellular repair mechanisms as expression increased for protein synthesis, fatty acid/lipid metabolism, and myelin genes. Genes involved in fatty acid/lipid metabolism were primarily modulated upward at 30 minutes, but downward modulation of genes occurred at 4 hours (table 2). Changes in such genes may be a response to IR-induced damage of cellular membranes. Additional support lies in the activation of the redox gene *Gpx4* which is involved in inhibiting lipid peroxidation after radiation exposure (Yant et al. 2003). Increased expression of genes coding for general ribosomal proteins at 4 hours suggest an increase in protein synthesis activity, which may be involved in activation of reparative

mechanisms within the cell (Zheng et al. 2001). Ribosomal proteins have also been implicated in a number of other functions, including regulation of cell-cycle control and apoptosis (Wool 1996, Chen and Ioannou 1999). We have observed increased expression of transcript coding for ribosomal proteins like L23a (table 2), which have been associated with inhibition of cell death (Lopez et al. 2002). The increase in myelin associated genes at 4 hours (table 4) suggest that low-dose IR affects the oligodendrocyte population responsible for myelin production. These increases may be a response to IR-induced damage to white matter that results in demyelination at higher doses (Ludwig et al. 1987, Kurita et al. 2001).

The changes observed in cell-cycle control and DNA synthesis genes suggest that low-dose irradiation may induce changes in cell-cycle control to allow damage repair to occur as observed at higher doses (Korr et al. 1989, Szumiel 1998). We observed increased expression for *Parp-2* which is involved in damage sensing mechanisms (Saxena et al. 2002), *Gas2*, a growth arrest specific gene, and *Pcna*, which is known to be involved in DNA synthesis activity (Paunesku et al. 2001). Both *Pcna* (Xu et al. 1998, Bishay et al. 2001, Uberti et al. 2001) and *Parp-2* (Doucet-Chabeaud et al. 2001) are known to be modulated in response to IR in other model systems. Increased expression of *Gas2* has been associated with growth arrest (Brancolini et al. 1992, Collavin et al. 1998), but other checkpoint genes like *Bub3* were down modulated, placing the involvement of growth arrest after low-dose exposure in question. Low-dose IR increased the expression of only a few DNA repair genes (e.g. *Xpa* and *Rad23b*). Also, the DNA synthesis/repair and cell cycle genes observed after low-dose irradiation of lymphoid cells (Amundsen et al. 1999, Amundsen et al. 2000, Tusher et al. 2001) did not produce

notable effects in our brain study, which may again be due to differences between in vitro and in vivo responses (Khodarev et al. 2001), or a result of the radioresistant nature of the brain. The small number of changes in DNA repair genes suggests that pre-existing proteins may be sufficient to repair low-dose damage in the irradiated brain.

In cases where arrest does not lead to repair, irradiated cells may undergo apoptosis (Szumiel 1998). Apoptosis has been observed in isolated neurons at doses as low as 2 Gy starting at 4-6 hours after IR exposure (Gobbel et al. 1998). However, our study, provides little evidence in favor of apoptosis, as few apoptosis related genes were modulated. There was decreased expression of the CASP8 and FADD-like apoptosis regulator *Cflar*, and increased expression of the programmed cell-death gene *Pdcd6* (table 2), but no change in the caspase genes like *Casp 3* (data not shown) that have been shown to be modulated during apoptosis of certain neuron populations (Chiang et al. 2001).

Our study suggests that low-dose IR induced a reduction of neuronal signaling activity, as evidenced by the down-modulation of transcription factors and genes involved in ion regulation, signal transduction, and synaptic signaling (table 2-4). Cluster analysis suggested a linkage between alteration of neuronal signaling activity and signal transduction activity (see supplemental materials). Previous studies have shown that IR can affect neuronal activity directly, but typically at doses of 40 Gy and higher (Tolliver and Pellmar 1987, Pellmar et al. 1990). In our study, many of the glutamate receptor genes involved in synaptic signaling were down regulated, including *Grik5*, *Grin1*, and *Gria3*. Further evidence in favor of IR-induced reduction of synaptic activity includes down-modulation of motor protein and cytoskeletal element genes (table 2), which are involved in axonal transport (Vale et al. 1992), as well as genes associated with vesicle

trafficking (table 2) which play important roles in exo- and endocytosis for transport and secretion of neurotransmitters (Hall 1992). Glutamate receptors also play roles in developmental and synaptic plasticity mechanisms (Ritter et al. 2002, Song and Huganir 2002), and changes in transcript levels of several genes involved in brain development were also observed. The developmental genes *Dbn* and *Rln* were down-modulated after IR exposure, with the latter observation consistent with studies in embryonic rat neuronal models (Darmanto et al. 1998). We also observed an IR-induced decrease in expression of the cell adhesion molecule *Ncam*, which is also involved in neural development. Decreases in protein levels of *Ncam* have been observed after low-dose IR exposure in embryonic systems, and are associated with reduction of cell migration (Fushiki et al. 1996). Neurotrophic factors like *Fgf9*, *Psap* and *Gfra2* which are involved in modifying neural architecture were also down-modulated in our study.

There are several noteworthy attributes to our study design and analysis plan. Most prior microarray experiments employed simple designs, comparing the effects of one or more treatments to a control. Instead, we have employed a factorial design with multiple observations at four combinations of dose and time which allow for us to estimate simple dose and time effects as well as more complex interactions (Fisher 1971, Kerr et al. 2000, Kerr and Churchill 2001, Cui and Churchill 2003, Wu et al. 2003). Notably, our approach moved away from an F distribution to a permutation distribution to assess significance, as our data set had enough distinct permutations of treatment labels (approximately 1000) to generate a large number of possible p-values. Smaller data sets like those in Tusher et al. (2001) have difficulties using permutation distributions directly due to the small number of potential re-labelings for treatments. We also adjusted for multiple comparisons in

order to control the false discovery rate, using the Benjamini-Hochberg procedure, which remains valid under positive dependence of the type encountered in microarray experiments where genes may be co-regulated (Reiner et al. 2001, Dudoit et al. 2002, Ge et al 2003). More sophisticated adjustment procedures (e.g. Benjamini et al. 2001) were also evaluated, but no dramatic differences in adjustment were noted. Future evaluations of factorial designs might include Bayesian approaches to compute the odds of differential expression, (Efron et al. 2001, Lonnstedt and Speed 2002). Lastly, the commercial genechips used in this study contained a large set of randomly selected genes, thus providing a near-global view of the low-dose IR-response that was not prejudiced in favor of pre-conceived cellular functions or biochemical pathways.

There are also several inherent limitations in the interpretation of our findings. First, this was a study of the adult male brain and it is not yet known how well the results can be generalized across age, sex, tissue type or species. Second, the FDR cut-value is a variable whose selection influenced the relative distribution of the 1574 IR-modulated genes into the four major response groups. For example, if stringency were increased by lowering the FDR, more genes shift into the independent-effect groups. In other words, if we had used an FDR of 0.15 (rather than the 0.20 used in our study), the number of genes classified as dose- and time-independent would have risen from 225 to 360 (figure 1, group 1), whilst the number of genes with a time-dependent effect would have decreased from 903 to 803 (group 2). The effect, however, was minimal for genes with dose-dependent effects, which changed from 79 to 77 (group 3). More dramatically, had we lowered the FDR to 0.10, the number of genes classified as dose and time independent would have risen to 666 (group 1), and the number of genes with a time-

dependent effect would have dropped to 606 (group 2), while no genes would have been classified into the two dose-dependent groups (groups 3 and 4). Lastly, over 300 of the genes that exhibited modulated expression in this study have not yet been annotated by name or function, and thus are a valuable future resource towards a more complete understanding of the response of the brain to low-dose irradiation.

There remains uncertainty in clinical implications of why so many genes are modulated after low-dose exposure and why some are modulated only at 0.1 Gy while others only at 2 Gy. IR exposures in the 0.1-0.5 Gy range has been previously shown to affect the developing brain in utero, reducing the brain size and intelligence of affected children (Schull et al. 1990, Devi et al. 1994, Kimler 1998), but little is known of the acute and long-term effects of low dose exposure to the adult brain. Interestingly, our set of 0.1 Gy exclusive genes includes the synaptic signaling, genes *Pclo*, *Gria1*, *Slcal* (table 2), *Cpneb*, *Gad2* and *Vtilb* (figure 3). *Gria1*, an AMPA1 glutamate receptor is of particular interest, as glutamate is the predominant excitatory neurotransmitter in the brain (Petrov 2002), and decrease in its expression levels may be involved in the depression of behavior previously observed in mice exposed to similar low doses (Miyachi et al. 1994, Miyachi and Yamada 1994). We also found an increase in *Irf3*, a major interferon regulatory factor (Levy et al. 2003) which may be involved in late-onset changes in mood and behavior after irradiation. Finally, it remains to be determined which of the induced transcript changes are indicators of enhanced protection and repair of cellular injury, and which portend clinically significant effects akin to the acute and late radiation injury seen after higher doses (Anno et al. 1989, Somosy 2000, Tofilon and Fike 2000).

**Acknowledgements:** We would like to thank Shalini Mabery, Dr. Francesco Marchetti, Dr. Xiu Lowe and Dr. Eddie Slotter for their assistance in the preparation of this manuscript. This work was performed under the auspices of the U.S. DOE by the University of California, LLNL contract W-7405-ENG-48.



## References

- ABAYOMI, O. K., 2002, Pathogenesis of cognitive decline following therapeutic irradiation for head and neck tumors. *Acta Oncologica*, **41**, 346-351.
- AMUNDSON, S. A., BITTNER, M., MELTZER, P., TRENT, J. FORNACE, A. J. JR., 2001, Induction of gene expression as a monitor of exposure to ionizing radiation. *Radiation Research*, **156**, 657-661
- AMUNDSON, S. A., DO, K. T., SHAHAB, S., BITTNER, M., MELTZER, P., TRENT, J., FORNACE, A. J. JR., 2000, Identification of potential mRNA biomarkers in peripheral blood lymphocytes for human exposure to ionizing radiation. *Radiation Research*, **154**, 342-346
- AMUNDSON, S. A., DO, K. T., FORNACE, A. J. JR., 1999, Induction of stress genes by low doses of gamma rays. *Radiation Research*, **152**, 225-231
- ANNO, G. H., BAUM, S. J., WITHERS, H. R., YOUNG, R. W., 1989, Symptomatology of acute radiation effects in humans after exposure to doses of 0.5-30 Gy. *Health Physics*, **56**, 821-838
- BELKA, C., BUDACH, W., KORTMANN, R. D., BAMBERG, M., 2001, Radiation induced CNS toxicity--molecular and cellular mechanisms. *British Journal of Cancer*, **85**, 1233-1239.
- BENJAMINI, Y., YEKUTIELI, D., 2001, The control of the false discovery rate under dependency. *Annals of Statistics*, **29**, 1165-1188

BISHAY, K., ORY, K., LEBEAU, J., LEVALOIS, C., OLIVIER, M. F., CHEVILLARD, S., 2000, DNA damage-related gene expression as biomarkers to assess cellular response after gamma irradiation of a human lymphoblastoid cell line. *Oncogene* **19**, 916-923

BOLSTAD, B. M., IRIZARRY, R. A., ASTRAND, M., SPEED, T. P., 2002, A comparison of normalization methods for high density oligonucleotide array data based on bias and variance. To appear in *Bioinformatics*.

BRANCOLINI, C., BOTTEGA, S., SCHNEIDER, C., 1992, Gas2, a growth arrest-specific protein, is a component of the microfilament network system. *Journal of Cellular Biology*, **117**, 1251-1261

CAO, Y., DULAC, C., 2001, Profiling brain transcription: neurons learn a lesson from yeast. *Current Opinions in Neurobiology*, **11**, 615-620

CHEN, F. W., IOANNOU, Y. A., 1999, Ribosomal proteins in cell proliferation and apoptosis. *International Review of Immunology*, **18**, 429-448

CHIANG, L.W., GRENIER, J. M., ETTWILLER, L., L. P. JENKINS, L. P., FICENEC, D., DISTEFANO, P. S., MARTIN, J., JIN, F., WOOD, A., 2001, Orchestrated gene expression component of neuronal programmed cell death revealed by cDNA array analysis. *Proceedings of the National Academy of Science, USA*, **98**, 2814-2819

CHIANG, C-S., HONG, J-H., STALDER, A., SUN, J-R., WITHERS, H. R., MCBRIDE, W. H., 1997, Delayed molecular responses to brain irradiation. *International Journal of Radiation Biology*, **72**, 45-53.

COLLAVIN, L., BUZZAI, M., SACCONI, S., BERNARD, L., FEDERICO, C., DELLAVALLE, G., BRANCOLINI, C., SCHNEIDER, C., 1998, cDNA characterization and chromosome mapping of the human GAS2 gene. *Genomics*, **48**, 265-269

CUI, X., CHURCHILL, G. A., 2003, Statistical Tests for Differential Expression in cDNA Microarray Experiments. Submitted to *Genome Biology*

DARMANTO, W., INOUE, M., HAYASAKA, S., TAKAGISHI, Y., OGAWA, M., MIKOSHIBA, K., MURATA, Y., 1998, Disturbed Purkinje cell migration due to reduced expression of Reelin by X-irradiation in developing rat cerebellum. *Biological Sciences in Space*, **12**, 254-255

DEVI, P. U., BASKAR, R., HANDE, M. P., 1994, Effect of exposure to low-dose gamma radiation during late organogenesis in the mouse fetus. *Radiation Research*, **138**, 133-138

DOUCET-CHABEAUD, G., GODON, C., BRUTESCO, C., DE MURCIA, G., KAZMAIER, M., 2001, Ionising radiation induces the expression of PARP-1 and PARP-2 genes in Arabidopsis. *Molecular Genetics and Genomics*, **265**, 954-963

DUDOIT, S., POPPER SHAFFER, J., BOLDRICK, J. C., 2002, Multiple hypothesis testing in microarray experiments, U.C. Berkeley Division of Biostatistics Working Paper Series, Working Paper 110, <http://www.bepress.com/ucbbiostat/paper11>

EFRON, B., TIBSHIRANI, R., STOREY, J. D., TUSHER, V., 2001, Empirical Bayes analysis of a microarray experiment. *Journal of the American Statistical Association*, **96**, 1151-1160

EISEN, M. B., SPELLMAN, P. T., BROWN, P. O., BOTSTEIN, D., 1998, Cluster analysis and display of genome-wide expression patterns. *Proceedings of the National Academy of Science U. S. A.*, **95**, 14863-14868

FEINENDEGEN, L. E., 2002, Reactive oxygen species in cell responses to toxic agents. *Human Experimental Toxicology*, **21**, 85-90

- FERRER, I., BARRON, S., RODRIQUEZ-FARRE, E., PLANAS, A. M., 1995, Ionizing radiation-induced apoptosis is associated with c-Jun expression and activation in the developing cerebellum of the rat. *Neuroscience Letters*, **202**, 105-108
- FISHER, R. A., 1971, The design of experiments, 8<sup>th</sup> edition (New York: Hafner)
- FUSHIKI, S., MATSUSHITA, K., YOSHIOKA, H. SCHULL, W. J., 1996, In utero exposure to low-doses of ionizing radiation decelerates neuronal migration in the developing rat brain. *International Journal of Radiation Biology*, **70**, 53-60
- GE, Y., DUDOIT, S., SPEED, T. P., 2003, Resampling-based multiple testing for microarray data hypothesis, Technical Report #633, Statistics Dept. University of California, Berkeley
- GOBBEL, G. T., BELLINZONA, M., VOGT, A. R., GUPTA, N., FIKE, J. R., CHAN, P. H., 1998, Response of postmitotic neurons to X-irradiation: implications for the role of DNA damage in neuronal apoptosis. *Journal of Neuroscience*, **18**, 147-155
- GOOD, P. I., 2000, Permutation Tests: A Practical Guide to Resampling Methods for Testing Hypotheses, 2nd edition (New York: Springer Verlag)
- HALL, Z. W., 1992, An Introduction to molecular neurobiology (Massachusetts: Sunderland)
- HONG, J. H., CHIANG, C. S., SUN, J. R., WITHERS, H. R., MCBRIDE, W. H., 1997, Induction of c-fos and junB mRNA following in vivo brain irradiation. *Molecular Brain Research*, **48**, 223-228
- HONG, J. H., CHIANG, C. S., CAMPBELL, I. L., SUN, J. R., WITHERS, H. R., MCBRIDE, W. H., 1995, Induction of acute phase gene expression by brain irradiation. *International Journal of Radiation Oncology, Biology, Physics*, **33**, 619-626

HOPEWELL, J. W., WRIGHT, E. A., 1970, The nature of latent cerebral irradiation damage and its modification by hypertension. *British Journal of Radiology*, **43**:161-167

IBUKI, Y., HAYASHI, A., SUZUKI, A., GOTO, R., 1998, Low-dose irradiation induces expression of heat shock protein 70 mRNA and thermo- and radio-resistance in myeloid leukemia cell line. *Biological Pharmaceutical Bulletin*, **21**, 434-439

IHAKA, R., GENTLEMAN, R., 1996, A language for data analysis and graphics. *Journal of Computational and Graphical Statistics*, **5**, 299-314

JOINER, M. C., MARPLES, B., LAMBIN, P., SHORT, S. C., TURESSON, I., 2001, Low-dose hypersensitivity: current status and possible mechanisms. *International Journal of Radiation Oncology, Biology, Physics*, **49**, 379-389

KANG, C-M., PARK, K-P., CHO, C-K., SEO, J-S., PARK, W-Y., LEE, S-J., LEE, Y-S., 2002, Hspa4 (HSP70) is Involved in the Radioadaptive Response: Results from Mouse Splenocytes. *Radiation Research*, **157**, 650–655

KAUFMAN, L., ROUSSEUW, P. J., 1990, Finding groups in Data: An Introduction to Cluster Analysis (New York: John Wiley & Sons)

KAWAKITA, Y., IKEKITA, M., KUROZUMI, R., KOJIMA, S., 2003, Increase of Intracellular Glutathione by Low-Dose g g -Ray Irradiation Is Mediated by Transcription Factor AP-1 in RAW 264.7 Cells. *Biological Pharmaceutical Bulletin*, **26**, 19-23

KERR, M. K., MARTIN, M., CHURCHILL, G. A., 2000, Analysis of variance for gene expression microarray data. *Journal of Computational Biology*, **7**, 819-837

KERR, M. K., CHURCHILL, G. A., 2001, Statistical design and the analysis of gene expression microarrays. *Genetical Research*, **77**, 123-128

- KHODAREV, N. N., PARK, J. O., YU, J., GUPTA, N., NODZENSKI, E., ROIZMAN, B., WEICHSELBAUM, R. R., 2001, Dose-dependent and independent temporal patterns of gene responses to ionizing radiation in normal and tumor cells and tumor xenografts. *Proceedings of the National Academy of Science, USA*, **98**, 12665-12670.
- KIM, S. H., LIM, D. J., CHUNG, Y. G., CHO, T. H., LIM, S. J., KIM, W. J., SUH, J. K., 2002, Expression of TNF-alpha and TGF-beta 1 in the rat brain after a single high-dose irradiation. *Journal of Korean Medical Science*, **17**, 242-248
- KIMLER, A. F., 1998, Prenatal irradiation: a major concern for the developing brain. *International Journal of Radiation Biology*, **73**, 423-434
- KORR, H., KOESER, K., OLDENKOTT, S., SCHMIDT, H., SCHULTZE, B., 1989, X-ray dose-effect relationship on unscheduled DNA synthesis and spontaneous unscheduled DNA synthesis in mouse brain cells studied in vivo. *Radiation and Environmental Biophysics*, **28**, 13-26
- KURITA, H., KAWAHARA, N., ASAI, A., UEKI, K., SHIN, M., KIRINO, T., 2001, Radiation-induced apoptosis of oligodendrocytes in the adult rat brain. *Neurological Research*, **23**, 869-874
- LEVY, D. E., MARIE, I. I., PRAKASH, A., 2003, Ringing the interferon alarm: differential regulation of gene expression at the interface between innate and adaptive immunity. *Current Opinions in Immunology*, **15**, 52-58.
- LONNSTEDT, I., SPEED, T. P., 2002, Replicated microarray data. *Statistica Sinica*, **12**, 31-46
- LOPEZ, C. D., MARTINOVSKY, G., NAUMOVSKI, L., 2002, Inhibition of cell death by ribosomal protein L35a. *Cancer Letters*, **180**, 195–202.

LUDWIG, R., CALVO, W., KOBER, B., BRANDEIS, W. E., 1987, Effects of local irradiation and i.v. methotrexate on brain morphology in rabbits: early changes. *Journal Cancer Research and Clinical Oncology*, **113**, 235-240

MACCALLUM, D. E., HALL, P. A., WRIGHT, E. G., 2001, The Trp53 pathway is induced in vivo by low doses of gamma radiation. *Radiation Research*, **156**, 324-327

MIYACHI, Y., KASAI, H., OHYAMA, H., YAMADA, T., 1994, Changes of aggressive behavior and brain serotonin turnover after very low-dose X-irradiation of mice. *Neuroscience Letters*, **175**, 92-94

MIYACHI, Y., YAMADA, T., 1994, Low-dose X-ray-induced depression of sexual behavior in mice. *Behavioral Brain Research*, **65**, 113-115

OGAWA, Y., SAIBARA, T., TERASHIMA, M., ONO, M., HAMADA, N., NISHIOKA, A., INOMATA, T., ONISHI, S., YOSHIDA, S., SEGUCHI, H., 1996, Sequential alteration of proto-oncogene expression in liver, spleen, kidney and brain of mice subjected to whole body irradiation. *Oncology*, **53**, 412-416

PANG, Z. P., DENG, P., RUAN, Y. W., XU, Z. C., 2002, Depression of fast excitatory synaptic transmission in large aspiny neurons of the neostriatum after transient forebrain ischemia. *Journal of Neuroscience*, **22**, 10948-10957

PAUNESKU, T., MITTAL, S., PROTIC, M., ORYHON, J., KOROLEV, S. V., JOACHIMIAK, A., WOLOSCHAK, G. E., 2001, Proliferating cell nuclear antigen (PCNA): ringmaster of the genome. *International Journal of Radiation Biology*, **77**, 1007-1021

- PELLMAR, T. C., SCHAUER, D. A., ZEMAN, G. H., 1990, Time- and dose-dependent changes in neuronal activity produced by X radiation in brain slices. *Radiation Research*, **122**, 209-214
- PETERSON, L. E., 2002, Factor analysis of cluster-specific gene expression levels from cDNA microarrays. *Computer Methods and Programs in Biomedicine*, **69**, 179-188.
- PETROFF, O. A., 2002, GABA and glutamate in the human brain. *Neuroscientist*, **8**, 562-573
- POLLARD, K. S., VAN DER LAAN, M. J., 2002, Identification of significant clusters in gene expression data. *Proceedings of the Joint Statistical Meetings*, August 2002, New York
- RAJU, U., GUMIN, G. J., TOFILON, P. J., 1999, NF kappa B activity and target gene expression in the rat brain after one and two exposures to ionizing radiation. *Radiation Oncology Investigations*, **7**, 145-152
- REINER, A., YEKUTIELI, D., BENJAMINI, Y., 2001, Identifying differentially expressed genes using false discovery rate controlling procedures. Accepted by *Bioinformatics*
- RITTER, L. M., VAZQUEZ, D. M., MEADOR-WOODRUFF, J. H., 2002, Ontogeny of ionotropic glutamate receptor subunit expression in the rat hippocampus. *Developmental Brain Research*, **139**, 227-236
- SAXENA, A., WONG, L. H., KALITSIS, P., EARLE, E., SHAFFER, L. G., CHOO, K. H., 2002, Poly(ADP-ribose) polymerase 2 localizes to mammalian active centromeres and interacts with PARP-1, Cenpa, Cenpb and Bub3, but not Cenpc. *Human Molecular Genetics*, **11**, 2319-2329.



- SCHULL, W. J., NORTAON, S., JENSH, R. P., 1990, Ionizing radiation and the developing brain. *Neurotoxicology and Teratology*, **12**, 249-260
- SERAFINI, T., 1999, Of neurons and gene chips. *Current Opinions Neurobiology*, **9**, 641-644.
- SHERLOCK, G., 2000, Analysis of large-scale gene expression data. *Current Opinions in Immunology*, **12**, 201-205
- SMYKAL, P., HRDY, I., PECHAN, P. M., 2000, High-molecular-mass complexes formed in vivo contain smHSPs and HSP70 and display chaperone-like activity. *European Journal of Biochemistry*, **267**, 2195-2207
- SOMOSY, Z., 2000, Radiation response of cell organelles. *Micron*, **31**, 165–181
- SONG, I., HUGANIR, R. L., 2002, Regulation of AMPA receptors during synaptic plasticity. *Trends in Neuroscience*, **25**, 578-588.
- SONIS, S. T., SCHERER, J., PHELAN, S., LUCEY, C. A., BARRON, J. E., O'DONNELL, K. E., BRENNAN, R. J., PAN, H., BUSSE, P., HALEY, J. D., 2002, The gene expression sequence of radiated mucosa in an animal mucositis model. *Cell Proliferation*, **35**, S93-102.
- STAMMLER, G., POMMERENKE, E. W., MASANEK, U., MATTERN, J., VOLM, M., 1996, Messenger RNA expression of resistance factors in human tumor cell lines after single exposure to radiation. *Journal of Experimental and Therapeutic Oncology*, **1**, 39-48
- SZUMIEL, I., 1998, Monitoring and signaling of radiation-induced damage in mammalian cells. *Radiation Research*, **150**, S92-101

TOFILON, P. J., FIKE, J. R., 2000, The radioresponse of the central nervous system: a dynamic process. *Radiation Research*, **153**, 357-370.

TOLLIVER, J. M., PELLMAR, T. C., 1987, Ionizing radiation alters neuronal excitability in hippocampal slices of the guinea pig. *Radiation Research*, **112**, 555-563

TUSHER, V. G., TIBSHIRANI, R., CHU, G., 2001, Significance analysis of microarrays applied to the ionizing radiation response. *Proceedings of the National Academy of Science U. S. A.*, **98**, 5116-5121

UBERTI, D., PICCIONI, L., CADEI, M., GRIGOLATO, P., ROTTER, V., MEMO, M., 2001, p53 is dispensable for apoptosis but controls neurogenesis of mouse dentate gyrus cells following gamma-irradiation. *Molecular Brain Research*, **93**, 81-89

USENIUS, T., TENHUNEN, M., KOISTINAHO, J., 1996, Ionizing radiation induces expression of immediate early genes in the rat brain. *Neuroreport*, **7**, 2559-2563

VALE, R. D., BANKER, G., HALL, Z. W., 1992, The Neuronal Cytoskeleton. In *An Introduction to molecular neurobiology*, edited by Z. W. Hall (Massachusetts: Sunderland), pp. 247-279

VAN DER KOGEL, A. J., The cellular basis of radiation induced damage in the CNS. In: *Cytotoxic Insult to Tissues: Late Effects on Cell Lineages*, edited by D. X. Potten and J. H. Hendry (Edinburgh: Churchill-Livingstone), pp. 329-352

VIAL, S., LU H., ALLEN, S., SAVORY, P., THORNTON, D., SHEEHAN, J., TOKATLIDIS, K., 2002, Assembly of Tim9 and Tim10 into a Functional Chaperone. *Journal of Biological Chemistry*, **277**, 36100–36108

- WAN, H., GONG, S. L., LIU, S. Z., 2001, Effects of low dose radiation on signal transduction of neurons in mouse hypothalamus. *Biomedical and Environmental Sciences*, **14**, 248-255
- WOOL, I. G., 1996, Extraribosomal functions of ribosomal proteins. *Trends in Biochemical Science*, **21**, 164–165
- WU, H., KERR, K., CHURCHILL, G. A., 2003, MAANOVA: A Software Package for the Analysis of Spotted cDNA Microarray Experiments. In *The Analysis of Gene Expression Data: Methods and Software*, G. Parmigiani, E. S. Garrett, R. A. Irizarry, S. L. Zeger (New York: Springer-Verlag)
- XU, J., MORRIS, G. F., 1999, p53-mediated regulation of proliferating cell nuclear antigen expression in cells exposed to ionizing radiation. *Molecular and Cellular Biology*, **19**, 12–20
- YANT, L. J., RAN, Q., RAO, L., VAN REMMEN, H., SHIBATANI, T., BELTER, J. G., MOTTA, L., RICHARDSON, A., PROLLA, T. A., 2003, The selenoprotein GPX4 is essential for mouse development and protects from radiation and oxidative damage insults. *Free Radical Biology and Medicine*, **34**, 496-502
- ZHENG, J. Q., KELLY, T. K., CHANG, B., RYAZANTSEV, S., RAJASEKARAN, A. K., MARTIN K. C., TWISS, J. L., 2001, A functional role for intra-axonal protein synthesis during axonal regeneration from adult sensory neurons. *Journal of Neuroscience*, **21**, 9291-9303.

**Table 1.** Distribution genes exhibiting modulation of expression after IR exposure.<sup>a</sup>

Modulation of expression		30 Minutes				4 Hours			
Fold-change	Direction	0.1 Gy exclusive	0.1 & 2 Gy	2 Gy exclusive	Total	0.1 Gy exclusive	0.1 & 2 Gy	2 Gy exclusive	Total
$\geq 1.5$	Up	102	163	69	334**	109	134	153	396***
	Down	105	257	63	425**	82	165	60	307***
$\geq 1.8$	Up	57	67	26	150	50	35	59	144*
	Down	79	141	43	263	55	67	41	163*
$\geq 2.0$	Up	33	36	18	77	21	18	30	69
	Down	67	93	39	199	46	37	28	111
$\geq 3.0$	Up	4	3	5	12	2	2	3	7
	Down	24	16	9	49	4	4	6	14

\* One gene not included in the total was down-modulated  $\geq 1.8$  at 0.1 Gy and up-modulated  $\geq 1.8$  at 2 Gy

\*\* Two genes not included in the total were up-modulated  $\geq 1.5$  at 0.1 Gy and down-modulated  $\geq 1.5$  at 2 Gy

\*\*\* Five genes not included in the total were up-modulated  $\geq 1.5$  at 0.1 Gy and down-modulated  $\geq 1.5$  at 2 Gy

<sup>a</sup> Each gene was assigned to one of three dose categories at each time point if the criteria for fold-change was met.

**Table 2. Genes related to general functions modulated by IR exposure**

Functional category	Patterns 1A, 3A, 3C	Patterns 1B, 3B, 3D	Pattern 2A	Pattern 2B	Pattern 2C	Pattern 2D
Catabolism	Psm4* (1.8) Ntan1* (1.7)	Capn2 (-1.8)	Lap3 (2.1) Ube2e1 (2.0) Lamp2 (1.9) Psm1 (1.9) Usp14 (1.7)	Ubb (-9.5) Ubd (-2.0) Uchl1 (-1.8) Ctsb (-1.6)	Rnase4 (1.7)	Ctsb (-1.8) Ubp2 (-1.7)
Cell-cycle control	Ptn (1.7) Tmsb4x (1.7) Csnk2a1-rs4** (2.3)	Ppm1g (-1.7)	Ccni (2.5) Rgs2 (2.2) Sept2 (2.0) Ptma (2.0) Gas2 (1.7) Cse1l (1.6) Tbc1d1 (1.6) Btg1 (1.5)	Calm2 (-4.9) Calm3 (-4.2) Anapc5 (-2.2) Fyn (-1.8) Csnk2a2 (-1.8) Bub3 (-1.7)	Sat (1.6) Cops3 (1.5) Pms2 (1.5) Rit2 (1.5) Sept4 (1.5)	Hcfc1 (-1.7) Pctk3 (-1.7) Kit (-2.0) Frap1 (-2.1) Bcl6 (-2.3)
Chromatin structure	Nap1l1* (1.8)	Brg1 (-2.2) Hdac6 (-1.6)	H3f3a (2.0) H3f3a (1.7) Hmgn2 (2.7)	Cbx1 (-2.3) Hdac7a (-2.3) Cbx5 (-1.5)	Baf53a (1.6) H3f2 (1.5)	
Cytokine/growth factor/ hormone	Il16 (2.0)	Fgf9 (-1.9)		Smst (-1.7)	Ogn (1.7)	
Cytoskeleton	Tln (1.7) Actb (1.5)		Actb (2.2) Arpc5 (1.6)	Enc1 (-7.5) Mtap2 (-3.5) Tuba6 (-2.6) Tuba2 (-2.5) Spm3 (-2.3) Eb2 (-2.0) Tubb5 (-1.7)	Tuba1 (1.5)	Tnnt2 (-3.4) Acta1 (-1.9) Tuba7 (-1.8)
Development		Dbn1 (-4.6) Reln (-2.3) Numb (-1.8)	Nm23 (1.9) Cd24a (1.7)		Zic1 (1.6) Nme2 (1.6)	Nrg1 (-2.6) Fliih (-1.5)
DNA synthesis/repair	Xpa (1.5)		Pole4 (2.5) Pcna (2.1)	Top1 (-1.8)		
ECM				Timp2 (-3.7) Bcan (-2.0)	Col11a2 (1.7)	Adam9 (-1.5) Plat (-1.8) Col11a2 (-1.5)
Heat shock	Dnajc8 (1.7)	Hsp70-2 (-2.5)	Dnajb9 (3.1) Hspe1 (1.9)	Hsp70-4 (-2.5), Hsp84-1 (-1.8)	Dnajb9 (1.8)	
Ion regulation/transport	Pva (1.6)	Atp1a1 (-4.0) Atp1a1 (-2.0)	S100a1 (2.2) S100a13 (1.9) Slc30a5 (1.8) Slc30a5 (1.6)	Atpv0a1 (-3.9) Spph1 (-2.3) Atp6v0c (-1.9) Kcnq2 (-1.9) Scn1b (-1.9) Atp6v1b2 (-1.5) Clcn3 (-1.6) Trpc1 (-1.6)	Scn1a (1.9) Atp6v0e (1.6) Fxyd1 (1.6) Atp5o (1.6) Pva (1.9)	Scn8a (-1.8) Slc30a3 (-1.5)
Metabolism (energy)	Timm8a* (2.1)	Pfkl (-2.0) Car14 (-1.5)		Pk3 (-2.0) Gpi1 (-2.2) Aco2 (-1.8) Gdm1 (-1.8) Slc25a14 (-1.8) Ckb (-1.6)	Hk1 (2.4)	Ccr4 (-2.0)
Metabolism (fatty acid/lipid)		Scd2 (-2.1)	Elovl2 (2.3) Scp2 (1.8) Gla (1.8)	Faah (-2.7) Dgat1 (-2.1)	Aldh1a1 (1.9)	
Metabolism (nucleoside/nucleotide)	Tmk (1.7)	Uck2 (-1.7)	Dck (1.6) Sucla2 (1.8)			

Motor protein		Dnm (-2.8)		Kif1a (-2.8) Dnm (-2.7) Myo5b (-1.6)		Myh9 (-1.8)
Protein synthesis	Eif1a (1.9) Mrpl54 (1.7) Srp14 (1.5) Mrpl45** (1.5)	Wars (-2.6) Large (-2.2) Eif2ak4 (-1.7) Siat7e (-1.7)	Naca (3.0) Rps5 (2.0) Mrpl11 (1.8) Mrps10 (1.6) Mrpl36 (1.6) Mrpl23 (1.5)	Pigq (-1.6) Arf3 (-3.8) Rpl7 (-1.8) Eef1a2 (-2.3) Fut9 (-2.6)	Eef1a1 (1.5) Rpl21 (1.5) Rpl28 (1.5) Rpl3 (1.5) Rps11 (1.5) Tign1 (1.5) Rpl27a (1.6) Rpl30 (1.6) Rps16 (1.6) Rps3 (1.6) Rps4x (1.6) Surf1 (1.6) Rpl23a (1.8) Rps6 (1.8) Rps7 (1.9) Mrps24 (1.8)	
Redox	Gpx4 (1.8) Cox6c (1.7) Ggh (1.7) Ndudaf1 (1.5)	Por (-2.3) Cox7a2l (-2.0)	Sod1 (2.0) Cycs (1.8) Cox4a (1.5)	Cyc1 (-1.7) Ppox (-1.5) Cox7c (-2.8)	Gstm5 (2.0) Prdx1 (1.8) Ndudfv2 (1.7) Cox7a3 (1.6)	
RNA synthesis/modification		Prp8 (-2.1)	Polr2I (2.3) U2af1 (2.0) Taf9 (1.9) Snrpa1 (1.8) Sfrs3 (1.6)	Srpk2 (-1.6) Elav13 (-2.2) Gtf2I (-2.3) Gtf2I (-2.6)		Ddx9 (-1.6)
Serum factors	Ttr (2.5) Bpgm (1.9)	Vtn (-3.3) Pfkp (-2.3) Slc4a3 (-2.0) Pfkp (-1.9)	Hbb-b2 (2.7)	Epb4.9 (-1.8) Mef2c (-2.4) Fgl2 (-1.7) Ly6h (-1.6)		
Signal transduction	Sh3d2c2 (2.4) Cd59a (1.6) Rab18 (1.6) Hs1bp1 (1.5) Hint* (1.6)	Ptpn13 (-1.5) Rassf5 (-1.6) Gnao (-1.7) Camk2b (-1.8) Igf1r (-2.0) Prkce (-2.0) Ptprn (-2.0) Prkcc (-2.8) Rhoip3 (-1.5) Nr4a2 (-1.6) Nr4a2 (-1.7) Pcdha5 (-1.8) Pcdh13 (-1.9) Nell2*** (-1.7) Il17r**** (-1.6)	Sh3d19 (2.8) Rala (2.1) Rab3d (2.0) Kail (1.7) Mc5r (1.7) Gabarapl2 (1.6) Gnai2 (1.6)	Rap2b (-1.5) Catna2 (-1.5) Traf3 (-1.5) Rock2 (-1.6) Ppia (-1.7) Grb10 (-1.7) Clk2 (-1.9) Mapk3 (-2.0) Cry2 (-2.0) Map3k3 (-2.1) Ptk91 (-2.4) Pla2 (-2.6) Prkar1b (-3.0) Tnk2 (-3.1) Dkk3 (-3.1) Ptpns1 (-5.2) Rab4b (-1.5) Ncor2 (-1.7) Pitpnb (-2.1) Prkar1b (-2.5) Rab7-ps1 (-1.6) Gnai1 (-1.7) Gng3 (-1.9) Nbr1 (-2.0) Arhgef7 (-2.6)	Arhgap5 (1.9) Arhn (2.2) Stk16 (1.6) Dtna (1.5) Lamr1 (1.9)	Ranbp9 (-1.6) Cdh2 (-1.6) Prkcb (-1.6) Rasa3 (-1.6) Smstr2 (-1.8) Adecy9 (-2.2) Ptpro (-1.8) Rasal1 (-2.0)
Transcription factor	Gtf3a (1.6)	Sox18 (-3.2) Cic (-2.8) Tp120a (-2.1) Jun (-1.8) Maged1 (-1.8)	Tcf7 (1.7) Tieg (1.7) Idb2 (1.9) Gtf2a2 (2.4) Idb4 (2.4) Tfdp1 (1.6)	Mt3 (-1.8) Madh2 (-1.6) Myt11 (-1.7) Mtf2 (-1.9) E4f1 (-2.0) Nono (-2.1) Mef2c (-2.2) Mef2c (-2.4) Dlx1 (-2.6) Zfp26 (-1.8)	Mt2 (1.6) Tcea1 (1.7) Tlp (2.1)	Zfp361l (-1.8) Nfix (-3.7) Yy1 (-1.6)

Vesicle trafficking	Snx2 (1.6)	Herc2 (-1.6) Nsf*** (-2.4)	Vmp (2.1) Stxbp3 (1.8)	Nf2 (-1.7) Sec8 (-1.7) Arf1 (-1.7) Vcp (-2.0) Napb (-2.1) Sec14l2 (-1.6) Epn1 (-2.2)	Vps29 (2.0)
---------------------	------------	-------------------------------	---------------------------	--	-------------

\* Gene modulated exclusively at 0.1 Gy (Pattern 3A)

\*\* Gene modulated exclusively at 2 Gy (Pattern 3C)

\*\*\* Gene modulated exclusively at 0.1 Gy (Pattern 3B)

\*\*\*\* Gene modulated exclusively at 2 Gy (Pattern 3D)

Numbers in parentheses represent the fold change of expression. Three functional categories which were not listed due to having fewer than five members, but which were of interest included the apoptosis genes Pdc6 (pattern 2A, 1.7-fold), Cflar (pattern 2B, -1.7-fold); inflammatory response genes C1qb (pattern 2A, 1.5-fold), C2 (pattern 2D, -2.9), Lta4h (pattern 3B, -1.7); and the cell adhesion genes Tjp1 (pattern 2D, -1.6), Ncam1 (pattern 2D, -1.9).

**Table 3. Genes related to neural/glia specific functions modulated by IR exposure**

Functional category	Patterns 1A, 3A, 3C	Patterns 1B, 3B, 3D	Pattern 2A	Pattern 2B	Pattern 2C	Pattern 2D
Myelin		Rtn4 (-1.9)		Rtn3 (-1.5)	Maobp (2.6) Mog (2.0) Plp (2.0) Mbp (1.6)	
Neurodegeneration		Sca2 (-1.8)		Apoe (-2.1) Prnp (-2.4) Cst3 (-1.8) App (-2.0)		
Synaptic signaling	Sybl1 (2.9)	Grin1 (-3.8) Pclo*** (-2.2) Gria1*** (-1.7) Slc1a1*** (-1.6)	Vamp4 (2.0) Gja1 (1.8) Sh3glb1 (1.7) Cplx2 (1.6)	Grik5 (-2.7) Homer1 (-1.6) Cck (-1.6) Ap1g1 (-1.7) Stx1a (-1.9) Gnas (-2.2) Dlgh4 (-3.4) Grin1 (-1.7) Ap1g1 (-6.9) Ap2a1 (-3.1) Syt5 (-2.1) Syt1 (-2.3) Syt11 (-2.5) Basp1 (-1.7) Epha7 (-1.8) Atp8a1 (-2.4) Cplx1 (-3.0) Gabarapl1 (-1.5) Gria3 (-1.9)		Ap2a2 (-1.9) Slc30a3 (-1.5)
<p>* Gene modulated exclusively at 0.1 Gy (Pattern 3A)</p> <p>** Gene modulated exclusively at 2 Gy (Pattern 3C)</p> <p>*** Gene modulated exclusively at 0.1 Gy (Pattern 3B)</p> <p>**** Gene modulated exclusively at 2 Gy (Pattern 3D)</p>						

Numbers in parentheses represent the fold change of expression. One functional categories which was not listed due to having fewer than five members, but which was of interest included the neurotrophin genes Psap (-10.1), Gfra2 (-8.5), Psap (-2.0) (2B).



**Table 4. Genes exhibiting complex patterns of expression after IR exposure**

<b>Functional category</b>	<b>Cluster 1 - Pattern 4A</b>	<b>Cluster 2 - Pattern 4B</b>	<b>Cluster 3 - Pattern 4C</b>
Catabolism	Capn3 (-1.4, -1.6/1.4, -1.1) Ube2l (-1.6, -1.3/-1.4, -1.0) Nedd4a (-1.7, -1.5/-1.4, -1.5) Smt3ip1 (-1.2, -1.1/-1.8, 1.0) Ube2e3 (-1.4, -1.1/1.1, -1.9)	Psmb7 (1.5, 1.4/1.4, 1.9) Psmb1 (1.7, 1.5/1.6, 2.1)	Poh1 (1.4, 1.5/1.1, 1.2) Uchl5 (1.6, -1.4/1.1, -1.2) Rbx1 (-1.1, 1.8/-1.2, 1.1)
Cell-cycle control	Csnk2a2 (-1.2, -1.5/-1.8, -1.3) Wig1 (-1.6, -1.5/-1.1, -2.1)	Fkbp2 (1.5, 1.1/1.4, 1.3) Nedd8 (1.5, 1.5/1.3, 1.8) S100a6 (1.7, 1.3/1.1, 1.9) Kip2 (2.0, 1.9/1.8, 1.3) Cops5 (1.4, 1.3/1.3, 1.6)	Tmsb10 (1.3, 1.3/1.1, 1.5)
Chromatin structure	Smarca1 (-2.9, -1.5/-1.6, -1.3)	H2afz (3.0, 1.5/2.1, 1.8) Zfp68 (2.1, 1.5/1.2, 1.8)	Smarca1 (-1.0, 1.2/1.3, 1.6) Supt4h2 (1.4, 1.3/1.1, 1.5)
Cytokine/growth factor/hormone	Igfbp5 (-2.0, -2.8/-1.4, -1.8) Amh (-1.9, -1.6/-1.5, -2.0)		
Cytoskeleton	Ank1 (-1.5, -1.4/-1.1, -1.7)		
DNA synthesis/repair	Rad23b (-1.2, -1.8/-1.0, -1.4) Adprt2 (-1.2, 1.1/-2.0, 1.4)		
ECM	Bgn (-1.1, -1.2/1.6, -1.4) Fbln1 (-1.6, -1.6/-1.3, -1.7)		Piga (1.3, 1.5/1.1, 1.6) Pigf (1.1, 1.7/1.2, 1.2)
Heat shock	Hsp86-1 (-1.8, 1.0/-1.3, 1.7)		
Inflammatory response	Nptx1 (-2.2, -2.1/-1.6, -2.2)		
Ion regulation/transport	Clen4-2 (1.1, -2.4/1.3, -1.0) Atp6v1a1 (-1.1, -1.7/-1.0, -1.0) Kena1 (-3.8, -2.0/-1.6, -1.2)	Clic4 (1.7, 1.4/1.5, 1.1)	
Metabolism (energy)	Pdha1 (-1.1, 1.0/-1.1, -1.6)	Atpi (1.8, 1.3/1.4, 1.5) Atp5c1 (2.0, 1.3/1.7, 1.9) Gatm (1.5, 1.2/1.5, 2.0) Timm23 (1.6, 1.3/1.4, 1.4) Timm10 (2.4, 2.0/1.7, 2.5)	
Metabolism (nucleoside/nucleotide)		Enpp2 (1.8, 1.2/2.4, 2.4)	
Motor protein	Dncic1 (-1.7, -1.6/-1.5, -1.3) Kif5a (-1.9, 1.9/-1.4, 1.2)		
Protein synthesis		Dpm1 (1.7, 1.1/1.4, 1.2) Rpl13a (1.7, 1.5/1.4, 1.9) Mrpl13 (1.7, 1.3/1.4, 1.7) Tgoln2 (1.5, 1.2/1.7, 1.7) Mrps21 (1.7, 1.5/1.2, 1.7)	Gp38 (-1.3, 1.1/1.3, 1.5) Rpl10a (1.4, 1.5/1.1, 1.7) Rps26 (1.2, 1.3/1.4, 1.7) Mrpl52 (1.4, 1.5/-1.0, 1.6)
Redox		Prdx3 (1.7, 1.2/1.6, 1.6) Ndubf9 (2.2, 1.6/1.6, 1.6) Hig1 (1.8, -1.1/1.2, 1.7) Txnl2 (2.2, 1.8/1.8, 1.9)	Cox5b (1.5, 1.2/1.1, 1.4) Txn1 (1.1, 1.3/-1.0, 2.0) Mgst3 (1.2, -1.0/-1.0, 1.6)
RNA synthesis/modification	Ddx6 2.5, 1.0/-1.3, 1.7)	Tceb1l (1.6, 1.4/1.3, 1.6) Snrpg (1.6, 1.6/1.1, 1.8) Sfrs3 (1.6, 1.6/1.1, 1.8)	
Serum factor		Ly6a (2.0, 1.5/1.6, 1.6)	Rbp1 (1.4, 1.3/1.3, 1.5) Fcgr1 (1.2, 1.0/1.8, -1.1)
Signal transduction	Plcb1 (1.0, -1.6/1.4, -1.0) Ptpn1 (-1.0, -1.7/1.0, 1.0) Dtx1 (-1.6, -1.6/-1.2, -1.9) Mapk9 (-2.1, 1.3/-1.7, 1.1) Cdh6 (-1.4, -1.2/-2.2, -1.6) Nisch (-2.0, -2.0/-2.6, -1.7) Arhgef1 (-1.6, -1.6/-2.6, -1.4)	Cdc42 (1.9, 1.6/1.6, 1.3) Resp18 (2.4, 1.5/1.7, 1.8) Gng10 (1.7, 1.5/1.5, 1.7)	Shd (1.2, 1.5/1.2, 1.1) Gna13 (1.2, 1.6/1.6, 1.3) Irak1 (1.1, 1.6/1.1, 1.2) Basp2 (1.5, 1.2/1.3, 1.3)
Synaptic signaling	Gabbr1 (-1.3, -1.6/-2.0, 1.2) Glr1 (-1.5, -1.1/-2.1, 1.4) Gad2 (-2.7, -1.1/1.0, -1.3) Cpne6 (-3.4, -2.6/-3.1, -3.3)	Vti1b (1.8, 1.4/1.4, 1.7)	Cript (1.3, 1.6/1.1, 1.3) Sh3glb1 (-1.2, 2.0/-1.1, 1.3)

Transcription factor	Madh1 (-1.1, -1.1/-1.1, -1.6)	Btf3 (2.6, 1.3/1.5, 1.4)	Irf3 (1.2, 1.8/1.6, 1.2)
	Tcfcp2 (1.0, 1.1/1.2, -1.6)	Shox2 (2.2, 2.4/3.5, 2.0)	Pbx1 (1.5, -1.1/1.2, 1.2)
	Hivep2 (-1.7, -1.6/-1.2, -2.2)		
	Tcf20 (-2.0, -1.6/1.1, 2.0)		
	Ash1 (-1.5, -1.4/-2.2, -1.1)		
Vesicle trafficking	Ap3b1 (-1.6, -1.2/-1.2, -1.3)		
	Slc16a2 (-1.6, -1.6/-1.1, -2.2)		

The first pair of numbers in parentheses represent 0.1 Gy at 30 min and 4 hr respectively, the second pair of numbers represent 2 Gy at 30 min and 4 hr respectively.

figure 1. Schematic of analysis plan for the selection and assignment of genes to dose- and time-dependent expression groups.

Out of the 9977 genes and ESTs (not including controls) on the arrays, 3517 had at least one positive signal in at least one chip ( $p < 0.01$ ). An F-ratio was calculated for detection of a difference in average signal intensity among any of the experimental groups, and 1574 genes which were detected at an FDR of 20%. Multifactorial analysis was then used to divide these genes into two categories based on dose dependency, and further subdivided into four groups according to their dose response patterns. Genes within each group were then tabulated by the magnitude of their fold-change (see supplemental material at the URL: <http://mcg.llnl.gov/external/supplemental/UCRL-JC-152221.htm> for more details).

figure 2. Genes showing IR induced changes in transcript levels by time and dose.

Using a fold-change threshold, genes with significant F-ratio were manually assigned to three dose response categories. From a total of nearly 10,000 genes, 759 were modulated at 30 minutes, while 703 were modulated at 4 hours by  $\geq 1.5$ -fold. At both time points there were exclusive sets of genes where modulation exceeded the fold change criteria for one dose, but not the other, suggesting qualitative differences in the responses at the two doses.

figure 3. Dose independent and dependent patterns of gene expression following IR exposure.

Multifactorial analysis assigned genes to separate expression pattern groups. Group 1 genes exhibited radiation responses that were not significantly different between 0.1 Gy and 2 Gy doses for both time points. Group 2 genes fell into four patterns that showed dependence upon time, but not dose. Group 3 genes fell into four patterns with significant differences between the two doses, but not time. The number of genes that exhibited each type of expression pattern are listed by increasing fold-change.

figure 4. Complex patterns of time and dose dependency.

PAM was used to cluster the 369 group 4 genes derived from multifactorial analysis into three major types of expression patterns. Two patterns of expression were time dependent for one dose, but time independent for the other (patterns 4A, 4B), and one pattern exhibited inverse time dependency for the two doses (pattern 4C).

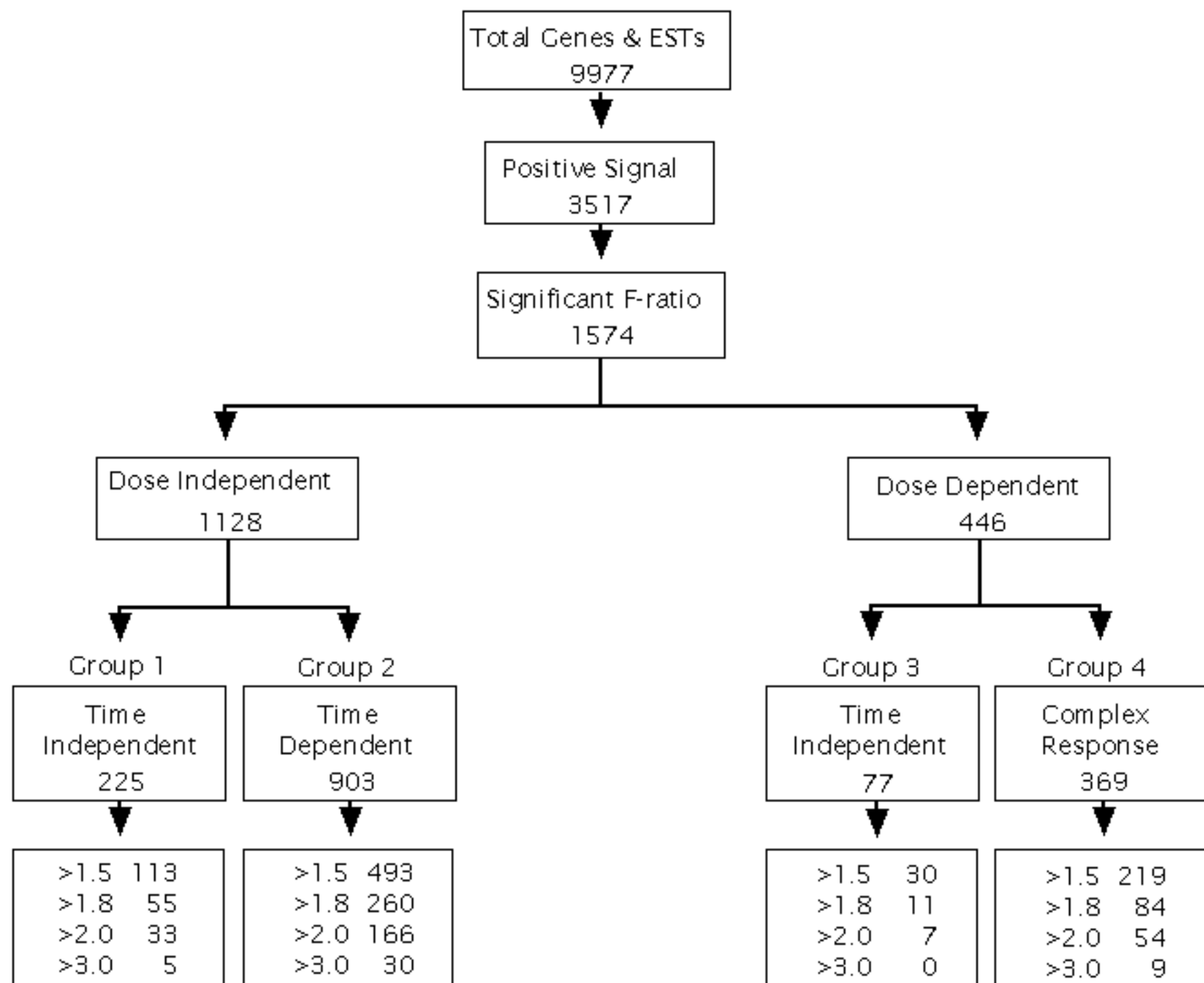
figure 5. Relative time-dependence of expression for genes in groups 1, 2 and 3.

The major patterns of gene expression were combined to show temporal relationships between pattern. Overall, the majority of genes were modulated at 30 minutes, showing either transient (patterns 2A, 2B) or sustained (patterns 1A, 1B, 3A-3D) patterns of expression. Genes which are transitorily modulated at 30 minutes, are followed by a different set of genes at 4 hours after IR exposure. Many IR-affected genes exhibited a decrease in transcript levels (figure 3, patterns 1B, 2B, 3B, 3D). Refer to tables 2-4 for the identity and functions of genes which follow these patterns.

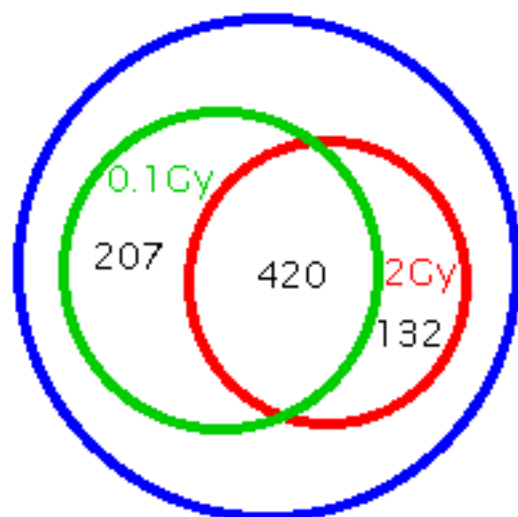
figure 6. Comparison of microarray and RT-PCR results.

Examples of genes showing time-dependence (*Pcna*) and dose-dependence (*Csnk2a1*, *Psma4*) by microarray analysis were examined by RT-PCR. Fold-changes for each experimental group were calculated by averaging the four possible combinations for fold-change (i.e. average of treatmentA/controlA, treatmentA/controlB, treatmentB/controlA, treatmentB/controlB). RT-PCR results are represented by diamonds, while microarray results are represented by squares. Error bars represent the standard deviation of RT-PCR and microarray results, drawn as single-sided bars.

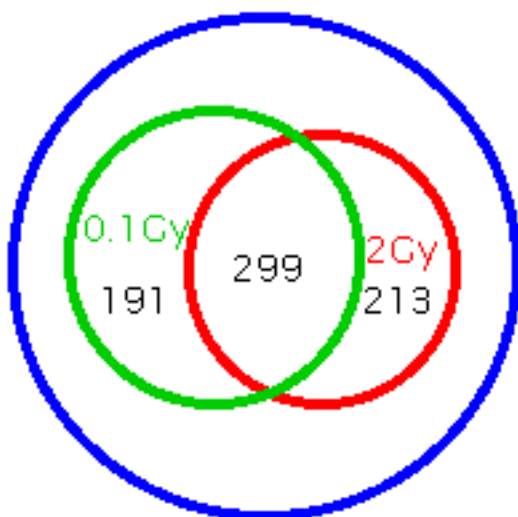




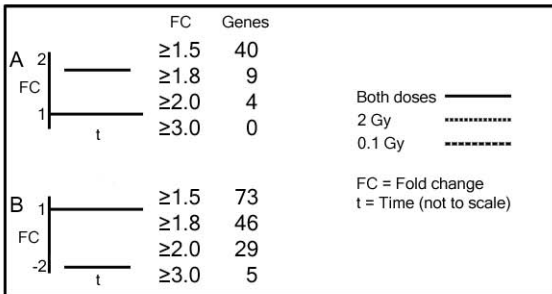
# A. 30 minutes



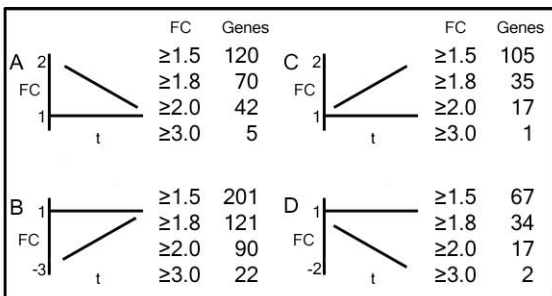
# B. 4 hours



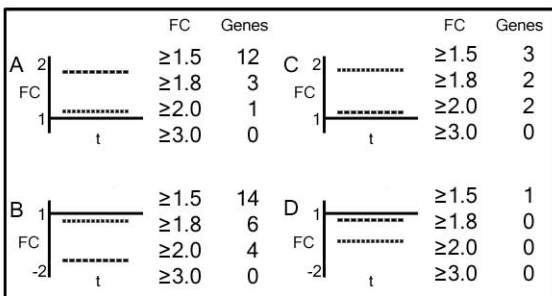
# A. Group 1 genes (dose and time independent)



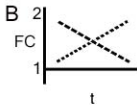
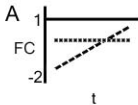
# B. Group 2 genes (time dependent)



# C. Group 3 genes (dose dependent, time independent)

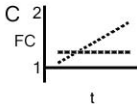


# Group 4 genes (complex)



Both doses —————

2 Gy .....  
0.1 Gy .....



FC = Fold change  
t = Time (not to scale)

